

Metal-insulator transition at 50 K in Na_2C_{60}

Y. Kubozono,* Y. Takabayashi, S. Fujiki, and S. Kashino
Department of Chemistry, Okayama University, Okayama 700-8530, Japan

T. Kambe
Department of Physics, Okayama University, Okayama 700-8530, Japan

Y. Iwasa
Japan Advanced Institute of Science and Technology, Ishikawa 923-1292, Japan

S. Emura
ISIR, Osaka University, Osaka 567-0047, Japan

(Received 14 October 1998; revised manuscript received 20 January 1999)

Temperature dependence of electron spin resonance in Na_2C_{60} was studied in a temperature range from 2 to 350 K. It was shown that Na_2C_{60} was metallic above 50 K and had a metal-insulator transition at 50 K. The center frequency for the Hg(2) Raman mode in Na_2C_{60} at 298 K was close to those in the metallic Rb_3C_{60} , K_3C_{60} , and Cs_3C_{60} , while the linewidth was close to that in the metallic but nonsuperconducting Cs_3C_{60} . The Hg(2) mode showed a large blueshift and narrowing at 50 K. The center frequency and the linewidth in the low-temperature region from 50 K were almost the same as those in the insulating C_{60} and Rb_6C_{60} , which showed the metal-insulator transition at 50 K in Na_2C_{60} . The origin of this metal-insulator transition was discussed in terms of the electron-phonon interaction (Jahn-Teller effect) and the electron-electron interaction (Mott-Hubbard picture). [S0163-1829(99)04123-5]

INTRODUCTION

The structure and physical properties of Na-doped C_{60} (Na_xC_{60}) are of very interest because they are different from those of the other alkali-doped C_{60} ($A_x\text{C}_{60}$, A :K, Rb, and Cs).¹⁻⁷ The superconducting phase has not yet been found for Na_xC_{60} ; Na_3C_{60} , which exhibits an face-centered cubic (fcc) structure ($Fm\bar{3}m$) is not a superconductor,¹ contrary to Rb_3C_{60} and K_3C_{60} . Na_xC_{60} with $x > 6$ can exist because of a small ionic radius of Na^+ ion; Yildirim *et al.* prepared $\text{Na}_{9.7}\text{C}_{60}$ with an fcc structure ($Fm\bar{3}$).² Recently, Oszlanyi *et al.* succeeded in preparing and characterizing Na_4C_{60} with two-dimensional polymer structure ($I2/m$); the C_{60} molecules were connected with "single" bonds.³ The structure is different from that of $A_4\text{C}_{60}$, which takes a body-centered tetragonal (bct) ($I4/mmm$) (Ref. 8) or a body-centered orthorhombic (bco) structure ($Immm$).⁹ In addition to these phases of Na_xC_{60} , the existence of two stable phases with an fcc structure ($Fm\bar{3}m$) is confirmed, which are Na_2C_{60} and Na_6C_{60} .^{1,4} The structure of Na_6C_{60} is different from a body-centered cubic (bcc) structure ($Im\bar{3}$) for $A_6\text{C}_{60}$.^{1,8} Furthermore, we recently reported the existence of NaC_{60} with an fcc structure.⁵

Early studies on the physical properties of Na_xC_{60} showed that these are insulating,^{10,11} except for one that reported a metallic behavior for Na_2C_{60} from the photoemission spectra.¹² Recently, Yildirim *et al.* reported the metallic behavior for Na_6C_{60} in the temperature region from 100 to 300 K on the basis of the spin susceptibility χ_{spin} determined from electron spin resonance (ESR).⁶ The polymeric phase of Na_4C_{60} also exhibited the metallic behavior.³ The χ_{spin} of

Na_4C_{60} ($1.7 \times 10^{-4} \text{ emu mol}^{-1}$) was smaller than that of RbC_{60} ($8 \times 10^{-4} \text{ emu mol}^{-1}$),³ suggesting a large bandwidth of Na_4C_{60} . Further, the high-temperature phase of Na_4C_{60} was metallic contrary to $A_4\text{C}_{60}$, although the phase took the same structure (bct, $I4/mmm$) as $A_4\text{C}_{60}$.⁷ The difference was rationalized on the basis of the Mott-Hubbard picture.^{7,13}

In the present paper, we report the metallic behavior of Na_2C_{60} and a metal-insulator (M-I) transition at 50 K on the basis of temperature-dependent ESR and Raman scattering. To our knowledge, this is the first experimental evidence for the M-I transition in Na_2C_{60} . Further, the electron-phonon coupling in Na_2C_{60} evaluated from Raman scattering is discussed in order to approach the origin of the M-I transition.

EXPERIMENT

The Na_2C_{60} sample was prepared by annealing stoichiometric amounts of C_{60} and Na metal for 856 h at 723 K under 10^{-3} Torr; a trace of benzene was removed before annealing. The nominal value of Na was 2.6. The sample was introduced into a quartz capillary tube for Raman and x-ray diffraction measurements, and an ESR tube for ESR and electron spin echo (ESE) measurements. The temperature-dependent ESR and ESE spectra were recorded at an x-band ESR spectrometer (Bruker ESP300) and Pulse Fourier-transform ESR spectrometer (Bruker ESP380E), respectively, equipped with an Oxford He flow Cryostat (ESR910). The temperature-dependent Raman spectra were measured by using an ISA Confocal LABRAM System equipped with an Oxford He flow Cryostat (Microstat-He) at an excitation of 632.8 nm with He-Ne laser: the spectral resolution was 5.0 cm^{-1} . The x-ray diffraction pattern was

measured with synchrotron radiation of $\lambda = 1.1010 \text{ \AA}$ at the BL-6C in the Photon Factory of High-Energy Accelerator Research Organization (KEK-PF). The differential scanning calorimetry (DSC) curve was recorded at the heating and cooling rates of 10 K min^{-1} with a Perkin-Elmer DSC7 calorimeter.

RESULTS

The Ag(2) Raman peak for the sample at 298 K showed the center frequency ω_0 of 1461 cm^{-1} . Comparison of the ω_0 with that reported for Na_xC₆₀ (Ref. 14) showed that this sample was Na₂C₆₀. The x-ray diffraction pattern at 298 K showed the same pattern as that for Na₂C₆₀ reported previously.⁴ The pattern was assigned to a simple cubic structure ($Pa\bar{3}$) and the lattice constant a was $14.19(1) \text{ \AA}$, consistent with that reported previously, 14.184 \AA .⁴ The a for Na₂C₆₀ was close to that for C₆₀ (14.17 \AA).¹⁵ The Rietveld analysis showed that the x-ray diffraction pattern could be reproduced with the atomic coordinates for the pristine C₆₀ at 5 K (Ref. 16) and $x = 0.236(6)$ for the Na atom on $8c$ site (x, x, x). The orientation of C₆₀ in Na₂C₆₀ determined in the present analysis was the same as that reported by Yildirim *et al.*⁴ The x value was close to that for Na₂CsC₆₀ ($x = 0.241$).¹⁷ This fact showed that the intercalation of Cs atom into $4b$ site ($\frac{1}{2}, \frac{1}{2}, \frac{1}{2}$) little affected to the position of Na atom on the $8c$ site. The DSC curve exhibited an endothermic peak at 325 K in a heating process. This peak can be assigned to the phase transition from the low-temperature simple cubic phase to the high-temperature fcc phase in Na₂C₆₀, as was reported by Yildirim *et al.*⁴ and Khairullin, Chang, and Hwang.¹⁸ No peaks except for this peak were observed in the DSC curve. These results showed that the sample was a single phase of Na₂C₆₀.

Figures 1(a), 1(b), and 1(c) show the ESR spectra for Na₂C₆₀ at 295 and 2 K, and the ESE spectrum observed in the field scan at 20 K, respectively. The spectrum at 295 K could be reproduced by using two Lorentzian functions with the peak-to-peak line widths ΔH_{pp} of 11.5 and 2.1 G. The spectrum was similar to that of NaC₆₀, which was composed of two components with ΔH_{pp} of 12.6 and 2.0 G at 263 K.⁵ These parameters were determined by a least-squares fitting with two Lorentzian functions. The ESR spectra were measured in a cooling process from 295 to 2 K, and in a heating process from 295 to 350 K. The ESE spectrum shown in Fig. 1(c) exhibited clearly the existence of two components with half linewidths $\Delta H_{1/2} (= \sqrt{3} \Delta H_{pp})$ of 11.6 and 4.9 G; the ΔH_{pp} of 6.7 and 2.9 G were consistent with those evaluated from ESR [Fig. 3(a)]. This result shows that the ESR spectrum should be analyzed by two components. The spectrum for Na₂C₆₀ at 2 K was also composed of two Lorentzian functions with ΔH_{pp} of 5.1 and 1.6 G.

As seen from Fig. 2(a), the temperature dependence of the χ_{spin} for the narrow component could be reproduced by Curie plus Pauli contributions; the Curie constant and χ_{spin} of the Pauli-type contribution were $1.60 \times 10^{-3} \text{ emu K mol}^{-1}$ and $0.424 \times 10^{-4} \text{ emu mol}^{-1}$, respectively. The Curie contribution was attributed to the paramagnetic defects in the crystals, as done for NaC₆₀.⁵ However, the origin of the small Pauli contribution found from the narrow ESR component was not clarified. As seen from Fig. 2(b), the broad compo-

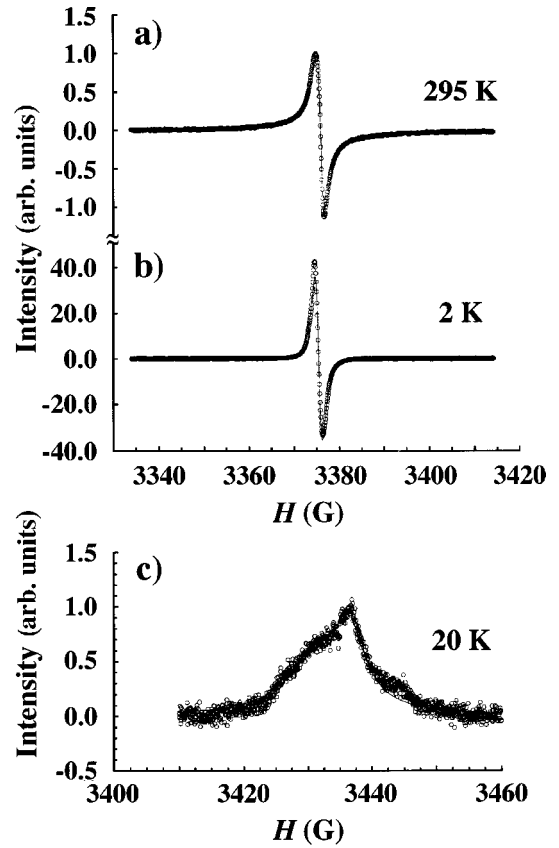


FIG. 1. ESR spectra of Na₂C₆₀ at (a) 295 and (b) 2 K. (c) ESE spectrum of Na₂C₆₀ at 20 K recorded in the field scan. The open circles and the solid lines refer to the experimental and the best-fitted spectra, respectively.

nent showed a Pauli-like behavior between 50 and 300 K, as a conventional metal. The χ_{spin} of the broad component decreased abruptly in the temperature region from 50 K. This change suggests the M-I transition at 50 K. The small decrease in the χ_{spin} of the narrow component between 20 and 50 K shown in Fig. 2(a) seems to be apparently observed owing to an abrupt decrease in the broad component. The χ_{spin} evaluated from the broad component was $1.3 \times 10^{-4} \text{ emu mol}^{-1}$ at 295 K, which was smaller than those for Rb₃C₆₀ ($12.7 \times 10^{-4} \text{ emu mol}^{-1}$),¹⁹ K₃C₆₀ ($9.3 \times 10^{-4} \text{ emu mol}^{-1}$) (Ref. 19) and Cs₃C₆₀ ($6.0 \times 10^{-4} \text{ emu mol}^{-1}$).^{20,21} The χ_{spin} of $1.3 \times 10^{-4} \text{ emu mol}^{-1}$ was consistent with that for Na₂C₆₀ at 290 K reported by Iwasa (ca. $1.5 \times 10^{-4} \text{ emu mol}^{-1}$).²² Further, the χ_{spin} was close to that for the polymeric Na₄C₆₀ at 300 K ($1.7 \times 10^{-4} \text{ emu mol}^{-1}$) and was a little smaller than that for the monomeric Na₄C₆₀ (ca. $4.0 \times 10^{-4} \text{ emu mol}^{-1}$).^{3,7} The density of state $N(\epsilon_F)$ on the Fermi level in Na₂C₆₀ was evaluated to be 2 state/eV-spin-C₆₀, which was smaller than those for Rb₃C₆₀ (19 state/eV-spin-C₆₀),¹⁹ K₃C₆₀ (14 state/eV-spin-C₆₀),¹⁹ and Cs₃C₆₀ (9 state/eV-spin-C₆₀).²¹ The small $N(\epsilon_F)$ suggests that the bandwidth W in the conduction band is larger for Na₂C₆₀ than those for Rb₃C₆₀, K₃C₆₀, and Cs₃C₆₀. The large W can reasonably be explained by the small a in Na₂C₆₀.

The sum of the χ_{spin} of two components shown in Fig. 2(c) exhibited an abrupt increase with a decrease in temperature at low temperatures because of the Curie-type contribu-

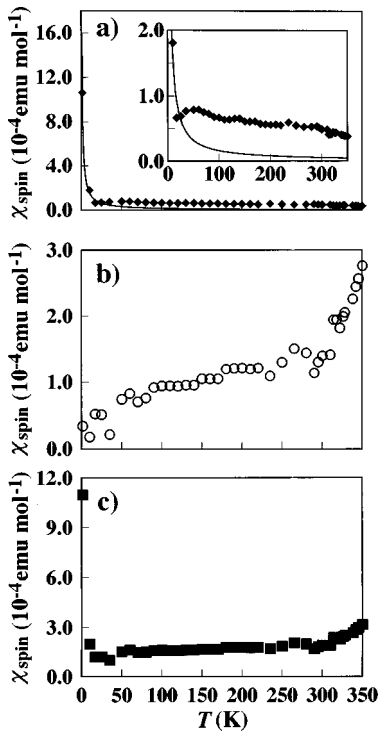


FIG. 2. Temperature dependence of the χ_{spin} evaluated from (a) the narrow ESR component, (b) the broad component, and (c) the sum of the broad and narrow components. The solid line in (a) shows the Curie contribution in the narrow component. The inset in (a) shows the χ_{spin} for the narrow components except for that at 2 K.

tion. A small decrease found between 20 and 50 K originates from an abrupt decrease in the χ_{spin} of the broad component. Though the total χ_{spin} for Na_2C_{60} reported by Iwasa showed the Curie-like behavior,²² the total χ_{spin} determined in the present study suggested the existence of some components other than the Curie-type component. The total χ_{spin} for Na_2C_{60} reported by Petit *et al.* showed the Curie-Weiss behavior (the Weiss temperature $\theta = 12$ K), and a drastic de-

crease below 10 K, which was assigned to the antiferromagnetic state.²³ As seen from Fig. 2(c), such a drastic decrease was not observed, though a small decrease in χ_{spin} was observed from 20 to 50 K. The χ_{spin} above 300 K showed an abrupt increase, which was consistent with the result reported by Petit *et al.*²³ They pointed out that the increase was caused by a singlet-triplet equilibrium of the spin states of C_{60}^{2-} dianion in Na_2C_{60} .²³ As seen from Figs. 2(a) and (b), the χ_{spin} of the broad component increased abruptly above 300 K, while the narrow component did not show such an increase. The fact suggests that the narrow component does not originate from the spin state of Na_2C_{60} .

As seen from Fig. 3(a), the ΔH_{pp} for the narrow component was almost constant below 300 K, while the component broadened slightly above 300 K. The ΔH_{pp} for the broad component was almost constant above 50 K, and decreased abruptly in the low-temperature region from 50 K. The results are very similar to those for NaC_{60} , except for the difference in the transition temperature: 280 K for NaC_{60} .⁵ The g factors for the narrow and broad components are shown in Fig. 3(b). The g factor for the narrow component was almost constant, while that for the broad component decreased below 50 K, suggesting the transition at 50 K. It was supported from the temperature dependence of the ΔH_{pp} and the g factor that the narrow component could primarily be attributed to the paramagnetic defects. The ΔH_{pp} for the broad component did not show a linear decrease with a decrease in temperature, as is expected for the conventional metal Rb_3C_{60} , which was metallic in the normal state above the superconducting transition temperature, showed an increase in ΔH_{pp} with decreasing temperature.²⁴ The peculiar temperature dependence of ΔH_{pp} was controversial because it was different from that in the conventional metal. Furthermore, the quadratic temperature dependence of the electric resistivity, which is closely associated with that of ΔH_{pp} , was also controversially discussed.^{25–27} Some proposals were presented based on the electron-electron scattering and the lattice contraction to explain this peculiar temperature dependence.^{24–27} However, Petit *et al.* found a decrease in

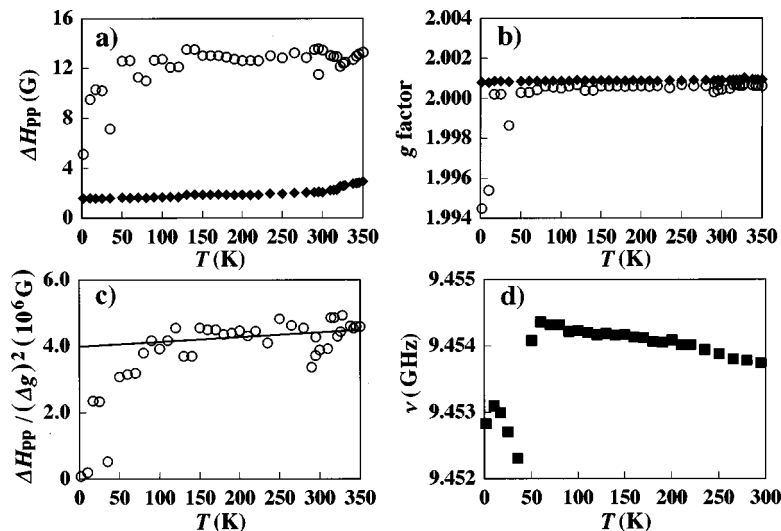


FIG. 3. (a) Temperature dependence of (a) the ΔH_{pp} and (b) g factor. The open circles and the rhombuses refer to the broad and the narrow components, respectively. (c) Temperature dependence of the $\Delta H_{pp}/(\Delta g)^2$ for the broad component. (d) Temperature dependence of the resonance frequency ν .

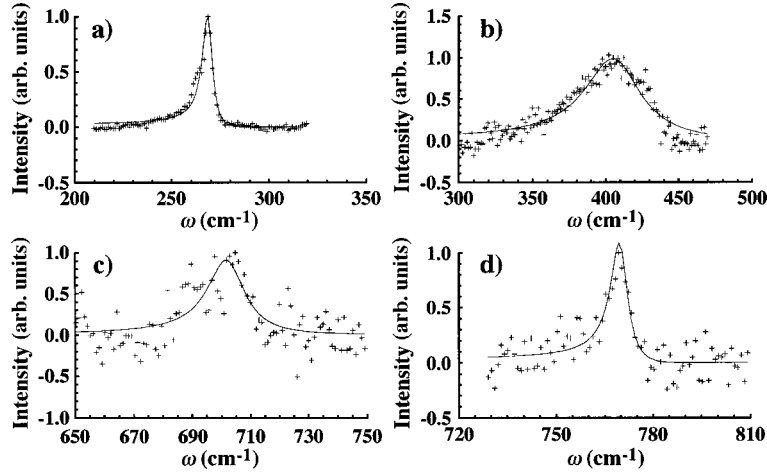


FIG. 4. Raman spectra for (a) the Hg(1), (b) Hg(2), (c) Hg(3), and (d) Hg(4) modes. The crosses and the solid lines refer to the experimental and the best-fitted Raman spectra, respectively. The fitting was carried out based on a single component.

the $\Delta H_{pp}/(\Delta g)^2$ when decreasing temperature: $\Delta g = g - 2.0023$.²⁸ The results could well be explained by the Elliott-Yafet relation for the conventional metal,^{29,30} implying that Rb₃C₆₀ was a metal above the superconducting transition.

Figure 3(c) shows the temperature dependence of the $\Delta H_{pp}/(\Delta g)^2$ in Na₂C₆₀ evaluated from the ΔH_{pp} [Fig. 3(a)] and the g factor [Fig. 3(b)] for the broad component. The temperature dependence showed a slight decrease in the $\Delta H_{pp}/(\Delta g)^2$ with a decrease in temperature above 50 K, suggesting the metallic character of Na₂C₆₀. The result implies that the dominant process for the spin-lattice relaxation in the broad ESR component is caused by the modulation of the spin-orbit interaction due to the lattice vibrations. However, the decrease was observed less clearly than that in Rb₃C₆₀. Consequently, it should also be pointed out that the other effects such as the electron-electron interaction may contribute to the temperature dependence of the ΔH_{pp} . The $\Delta H_{pp}/(\Delta g)^2$ also decreased abruptly in the low-temperature region from 50 K, suggesting the transition of the magnetic states. We have concluded from the Pauli-like χ_{spin} and the decrease in the $\Delta H_{pp}/(\Delta g)^2$ that Na₂C₆₀ is metallic above 50 K, and that the M-I transition occurs at 50 K. The broad component in Na₂C₆₀ was assigned to the conduction-electron ESR (c-ESR).

Figure 3(d) shows the temperature dependence of the resonance frequency ν in the ESR measurements. The ν increased monotonically with decreasing temperature above 50 K. Below 50 K the values decreased drastically. This drastic change reflects the change in the electric conductivity; the ν for materials which has no transition increases monotonically with a decrease in temperature. Therefore, the temperature dependence of the ν also supports the M-I transition in Na₂C₆₀ around 50 K.

Figures 4(a), 4(b), 4(c), and 4(d) show the Raman spectra for the Hg(1), Hg(2), Hg(3), and Hg(4) observed at 298 K. The center frequency ω_0 , the width Γ , and the asymmetric parameter q were determined by a least-squares fitting with Breit-Wigner-Fano formula; the fitting was carried out with a single component. These parameters are collected in Table I, together with those for the Ag(1) and Ag(2). Winter and Kuzmany analyzed the Hg(1) and Hg(2) peaks for a single

crystal of K₃C₆₀ by the five-components fitting,³¹ because their spectrometer with high-spectral resolution (3 cm⁻¹) showed splitting for these peaks. The fitting with the two components was carried out for the Hg(1) peak in Na₂C₆₀ since a small additional component was observed. Figures 5(a) and 5(b) show the Hg(1) peaks at 298 and 2 K, respectively, together with the two-components fitting-curves. This two-components fitting led to an improvement in the parameter fitting. The ω_0 , Γ , and q by the fitting are also listed in Table I. The weighted average values of the ω_0 , Γ , and q determined by the two-components fitting were consistent with those by a single-component fitting. The splitting in the Hg(2) peak was not clearly observed because of the spectral resolution of our Raman equipment and the polycrystalline sample. Thus, only a single-component fitting was employed in the analysis for the Hg(2) peak. The ω_0 , Γ , and q determined by a single-component fitting should correspond to the weighted average values for those determined by multi-components fitting.

The Γ for the Hg(2) mode at 298 K was extremely larger than those for the other modes. The Γ for the other modes in Na₂C₆₀ were comparable to those in C₆₀ at room

TABLE I. The values of ω_0 (cm⁻¹), Γ (cm⁻¹), q , and $\Delta\Gamma/\omega_0^2$ (10⁻⁵ cm) for Raman-active modes at 298 K in Na₂C₆₀. Parameters determined by a single-component fitting.

| Mode | Na ₂ C ₆₀ | | | | C ₆₀ ^a | |
|-------|---------------------------------|----------|-----|---------------------------|------------------------------|----------|
| | ω_0 | Γ | q | $\Delta\Gamma/\omega_0^2$ | ω_0 | Γ |
| Hg(1) | 269 | 3 | -7 | } ^b | 270 | 4.2 |
| | 269 | 2 | -17 | | | |
| | 263 | 4 | -13 | | | |
| Hg(2) | 406 | 24 | -15 | 11 | 430.5 | 5.5 |
| Ag(1) | 492 | 3 | -35 | 0.06 | 493 | 2.5 |
| Hg(3) | 702 | 8 | -16 | 0.06 | 708 | 7.5 |
| Hg(4) | 770 | 3 | -7 | | 773 | 9.0 |
| Ag(2) | 1461 | 4 | 374 | 0.10 | 1469 | 1.5 |

^aParameters at 300 K taken from Ref. 32 (488 and 514.5 nm excitation).

^bParameters determined by two-components fitting.

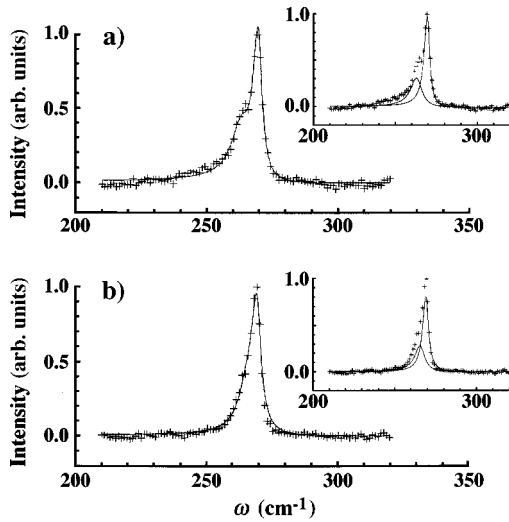


FIG. 5. Raman spectra for the Hg(1) mode at (a) 298 and (b) 2 K. The crosses and the solid lines refer to the experimental and the best-fitted Raman spectra, respectively. The fitting was carried out based on two components. Two components are drawn with the solid line in the inset with the experimental spectrum.

temperature.^{21,32} Consequently, it was suggested that the interaction between the electron and intramolecular Hg(2) phonon was very strong. The electron phonon coupling constant λ for the Hg(2) mode was evaluated to be 0.7 from the $\Delta\Gamma/\omega_0^2$ of 11.0×10^{-5} cm and the $N(\epsilon_F)$ of 2 state/eV-spin- C_{60} according to $\lambda_i = C\Delta\Gamma_i/[\omega_{0i}^2 N(\epsilon_F)]$ and $\Delta\Gamma_i = \Gamma_i(\text{Na}_2\text{C}_{60}) - \Gamma_i(\text{C}_{60})$;^{33,34} the ω_{0i} is the ω_0 for the i th Raman mode and $C = d_i/\pi$, d_i being the degeneracy of the i th mode ($d_i = 5$ for Hg mode and $d_i = 1$ for Ag mode). The $\Gamma_i(\text{Na}_2\text{C}_{60})$ and $\Gamma_i(\text{C}_{60})$ are the linewidth Γ for the i th mode in Na_2C_{60} and C_{60} , respectively. The total $\lambda (= \sum \lambda_i)$ was 0.7, which was comparable to that in Rb_3C_{60} at room temperature ($\lambda = 0.5$).³² The total λ in Na_2C_{60} is primarily contributed from the Hg(2) mode.

The $1/q$ implies the strength of the coupling between the continuum and the discrete modes. If the continuum is assigned to the electronic origin rather than vibrational, the $1/q$ can become a measure of the coupling strength of each mode with the electrons which participate in the electronic transition.^{32,35} The origin of the continuum around Hg(2) in Rb_3C_{60} was assigned to the interband $t_{1u} - t_{1u}^*$ transitions.^{32,35} The three degenerate t_{1u} orbitals in C_{60} form the conduction band, and the transition energy of the interband $t_{1u} - t_{1u}^*$ was expected to be as small as 0.1 eV from the band-structure calculation,³⁶ so that the interband transition can be excited by the Hg(2) Raman scattering process. Therefore, the $1/q$ for the Hg(2) mode is a measure of the coupling to the t_{1u} conduction electrons. The $1/q$ of -0.07 for the Hg(2) mode at 298 K suggests the intense coupling. Further, the negative value of $1/q$ implies that the ω_0 for the electronic continuum lies below the ω_0 for the Hg(2) mode.

Figures 6(a), 6(b), and 6(c) show the the Raman spectra for the Hg(1), Hg(2), and Hg(4) observed at 2 K. The clear blueshift of ω_0 and the narrowing in Γ for the Hg(2) peak at 2 K can be found in comparison with those at 298 K. On the other hand, the clear changes were not observed for the Hg(1) and Hg(4) peaks. The ω_0 , Γ , and q for the Hg and Ag

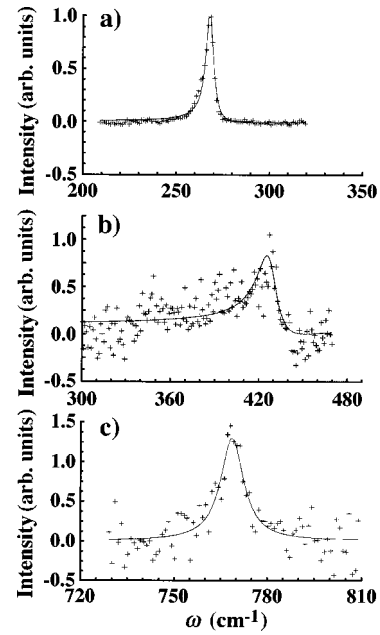


FIG. 6. Raman spectra for (a) the Hg(1), (b) Hg(2), and (c) Hg(4) modes. The crosses and the solid lines refer to the experimental and the best-fitted Raman spectra, respectively. The fitting was carried out based on a single component.

modes at 2 K are listed in Table II. Figures 7(a), 7(b), and 7(c) show the temperature dependence of the ω_0 , Γ , and q for the Hg(2) mode in Na_2C_{60} . The ω_0 showed a drastic blueshift at 50 K; the ω_0 was approximately 410 cm^{-1} above 70 K, while the ω_0 approximately 430 cm^{-1} at 50 K and the temperatures lower than 50 K. The ω_0 above 70 K is close to those observed at room temperatures for Rb_3C_{60} (395 cm^{-1} at 300 K,³² 408 cm^{-1} at 300 K),³⁷ K_3C_{60} (416 cm^{-1} at 300 K),³² and Cs_3C_{60} (406 cm^{-1} at 290 K),²¹ which show the metallic behavior; the excitation wavelengths were 488 and 514.5 nm for Refs. 32 and 37, and 632.8 nm for Ref. 21. The ω_0 for the Hg(2) mode observed by 1064 nm excitation were 435 cm^{-1} for Rb_3C_{60} and 430 cm^{-1} for K_3C_{60} (Ref. 35), which were largely different from those by 488 or 514.5 nm excitation.³⁵ The difference seems to originate from the large difference in the excitation wavelength. Consequently, the ω_0 for Na_2C_{60} obtained by 632.8 nm excitation cannot di-

TABLE II. The values of ω_0 (cm^{-1}), Γ (cm^{-1}), and q for Raman-active modes at 2 K in Na_2O_{60} . Parameters were determined by a single-component fitting.

| Mode | Na_2C_{60} | | |
|-------|----------------------------|----------|-------|
| | ω_0 | Γ | q |
| Hg(1) | 268 | 3 | -11 |
| | 269 | 2 | -42 |
| | 265 | 4 | -15 |
| Hg(2) | 428 | 8 | -3 |
| Ag(1) | 492 | 2 | -1969 |
| Hg(3) | | | |
| Hg(4) | 769 | 4 | -228 |
| Ag(2) | 1460 | 3 | 374 |

^aParameters determined by two-components fitting.

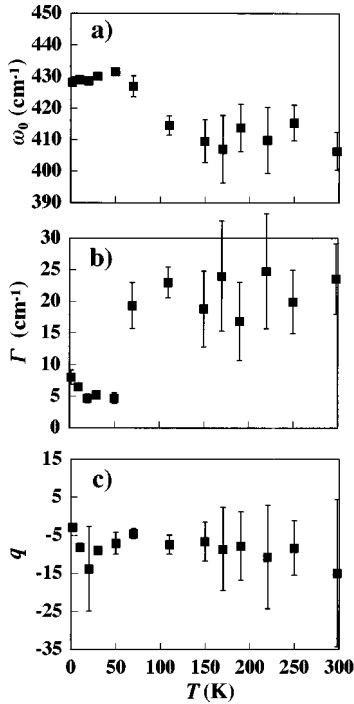


FIG. 7. Temperature dependence of (a) the ω_0 , (b) Γ , and (c) q for the Hg(2) mode.

rectly be compared with those in Ref. 35. The ω_0 observed in the temperature region from 50 to 2 K is consistent with those observed at room temperature for C₆₀ [430.5 cm⁻¹ at 300 K (Ref. 32)] and Rb₆C₆₀ [428 cm⁻¹ at 298 K (Ref. 21)] which show the insulating behavior. The Γ showed a drastic decrease at 50 K; the Γ was approximately 20 cm⁻¹ above 50 K, while the Γ was approximately 5 cm⁻¹ in the temperature region from 50 to 2 K. The Γ at the higher temperatures than 50 K is close to that for Cs₃C₆₀ at room temperature (16 cm⁻¹ at 290 K);²¹ the Γ for the superconducting K₃C₆₀ and Rb₃C₆₀ were 75 and 74 cm⁻¹ at 300 K, respectively,³² which were broader than that for the metallic but nonsuperconducting Cs₃C₆₀.²¹ On the other hand, the Γ in the temperature region from 50 to 2 K is close to those for the insulating C₆₀ [5.5 cm⁻¹ at 300 K (Ref. 32)] and Rb₆C₆₀ [4 cm⁻¹ at 298 K (Ref. 21)]. The temperature dependence of Γ indicates that the interaction between the electron and the intramolecular Hg(2) phonon in Na₂C₆₀ in the temperature region from 50 to 2 K is remarkably different from that above 50 K. We confirmed from the temperature dependence of the ω_0 and Γ that Na₂C₆₀ has the M-I transition at 50 K. The q was almost constant within the experimental error in all temperature region, and no drastic change was observed at 50 K. The reason why the q does not reflect the M-I transition at 50 K is not clear at the present stage. Recently, we observed almost the same q for the Hg(2) mode in the metallic Cs₃C₆₀ and the insulating Rb₆C₆₀, in spite of the absence of the $t_{1u}-t_{1u}^*$ transition for the insulating Rb₆C₆₀.²¹ These facts reflect the difficulty in the estimation of q value for the Hg(2) peak.

DISCUSSION

We examined some scenarios to account for the electronic state and the origin of the M-I transition in Na₂C₆₀. First, the

possibility of one or two-dimensional polymer was considered for Na₂C₆₀. If Na₂C₆₀ took the polymer structure, a descent in symmetry of the C₆₀ molecule from I_h to a low symmetry such as D_{2h} should lead to the large splitting of each Raman-active mode. The large splittings were actually observed for all Hg modes and Ag(2) mode when RbC₆₀ transformed from the monomeric phase to the polymeric one.^{38,39} Furthermore, we also observed the large splitting for the Hg(1), Hg(2), Hg(3), Hg(4), and Ag(1) peaks in the polycrystalline sample of polymeric RbC₆₀ at 298 K. However, such a large splitting was not observed for Na₂C₆₀ in the temperature region from 298 to 2 K, though the small splitting was observed for the Hg(1) peak; the Hg(1) peak in the polymeric RbC₆₀ consisted of at least three components and the splitting was larger than that in Na₂C₆₀.⁴⁰ This fact suggests that Na₂C₆₀ does not take a one-dimensional (1D) or two-dimensional (2D) polymeric structure in the temperature region. Consequently, it is difficult to attribute the M-I transition to the Peierls instability.

The second possibility was the Mott-Hubbard picture. The N -fold degenerate Hubbard model within the Gutzwiller approximation shows that the critical energy U_c , which separates an insulator from a correlated metal, sensitively depends on both the degeneracy and the electron-filling; the value of U_c is maximum at half filling ($U_c/W=2.62$ for $x=1$, 3.65 for $x=2$ and 4.00 for $x=3$ in A_xC_{60} with $N=3$).⁴¹ Consequently, it is difficult for a degenerate system to become a Mott-Hubbard insulator near half filling, because the large electron-electron Coulomb repulsion U is required.⁴¹ Thus, A_xC_{60} is expected to show a metallic behavior at $x=3$ and an insulating or metal-insulator transition at $x=2$ and 4.⁴¹ If Na₂C₆₀ has a slightly larger U/W than the U_c/W , it should be metallic above the critical temperature and insulating below the temperature. Such a scenario is presented for the high-temperature monomeric phase of Na₄C₆₀.^{7,13} Only the monomeric Na₄C₆₀ among A_xC_{60} with the bct structure was metallic because of the large W caused by the short interfullerene distance of 9.80 Å. This fact suggests that A_xC_{60} fullerides are the Mott-Hubbard insulators.^{7,13} The W for the Na₂C₆₀ is larger than that for the monomeric Na₄C₆₀ judging from the χ_{spin} . In spite of the larger W , Na₂C₆₀ was insulating in the low-temperature region from 50 K. This fact suggests the Mott-Hubbard picture with a large U for Na₂C₆₀.

Furthermore, the Jahn-Teller distortion was considered as the origin of the M-I transition, because the conduction band in Na₂C₆₀ is partially filled by an even number of electrons. The Hg(2) Raman peak for Na₂C₆₀ showed the strong electron-phonon coupling above the M-I transition temperature and the drastic change with the M-I transition. The strong electron-phonon coupling may be an indication of the Jahn-Teller distortion in Na₂C₆₀. Taliani *et al.* pointed out that the occurrence of the asymmetric Fano line shape in the Hg(2) Raman mode was due to the splitting of t_{1u} conduction band that originates from the Jahn-Teller distortion or other interactions.³⁵ The small gap in the conduction band caused by the Jahn-Teller distortion can lead to the metallic behavior at high temperature and the insulating behavior at low temperature.

The temperature dependent x-ray diffraction did not give the experimental evidence for the Jahn-Teller distortion of

the C_{60} molecule in Na_2C_{60} , and showed no clear structural change at 50 K; the temperature dependence of the a and the Debye-Waller factor of Na atom from 2 to 280 K were well fitted by the Grüneisen relation and the Debye approximation, and the Rietveld analyses for the x-ray diffraction patterns at 10 and 50 K could be performed with the same space group and the same orientation of C_{60} of I_h symmetry as those at 298 K. Therefore, the M-I transition for Na_2C_{60} seems to be a transition without the structural change. However, if the Jahn-Teller distortion is dynamical, it is difficult to detect the structural distortion even at low temperature. Though the rapid decrease in the χ_{spin} in the low-temperature region from 50 K supports the Mott-Hubbard transition, the decrease in the ΔH_{pp} in the temperature region is not consistent with the Mott-Hubbard insulator, which should show an increase in ΔH_{pp} because of the antiferromagnetic ground state. The behavior of the χ_{spin} and the ΔH_{pp} below the M-I transition seems to suggest the nonmagnetic ground state. If the M-I transition is attributed to the Jahn-Teller distortion, the ground state realized for the insulating Na_2C_{60} will be nonmagnetic.

In the present paper, it has been shown that the electronic

correlation and the Jahn-Teller effect should be considered to understand the origin of the M-I transition in Na_2C_{60} . The definitive evidence on the origin of the M-I transition will be given by the elucidation of the magnetic nature of the ground state below 50 K. When applying pressure to the insulating Rb_4C_{60} , this transformed to the metal under 8 kbar because of an increase in the W and the screening of the U .⁴² This fact implies that the M-I transition disappears by applying pressure, if Na_2C_{60} is the Mott-Hubbard insulator as A_4C_{60} . Furthermore, the large electron-phonon coupling in Na_2C_{60} , which is comparable to that in Rb_3C_{60} , may lead to the superconducting transition at low temperature, when the M-I transition disappears under pressure.

ACKNOWLEDGMENTS

The authors are grateful to Professor K. Tanigaki of Osaka City University and Professor K. Oshima of Okayama University for helpful discussions. This study was financially supported by the Venture Business Laboratory of Okayama University.

*Author to whom correspondence should be addressed.

- ¹M. J. Rosseinsky, D. W. Murphy, R. M. Fleming, R. Tycko, A. P. Ramirez, T. Siegrist, G. Dabbagh, and S. E. Barrett, *Nature (London)* **356**, 416 (1992).
- ²T. Yildirim, O. Zhou, J. E. Fischer, N. Bykovetz, R. A. Strongin, M. A. Cichy, A. B. Smith III, C. L. Lin, and R. Jelinek, *Nature (London)* **360**, 568 (1992).
- ³G. Oszlanyi, G. Baumgartner, G. Faigel, and L. Forro, *Phys. Rev. Lett.* **78**, 4438 (1997).
- ⁴T. Yildirim, J. E. Fischer, A. B. Harris, P. W. Stephens, D. Liu, L. Brard, R. M. Strongin, and A. B. Smith III, *Phys. Rev. Lett.* **71**, 1383 (1993).
- ⁵Y. Takabayashi, Y. Kubozono, S. Kashino, Y. Iwasa, S. Taga, T. Mitani, H. Ishida, and K. Yamada, *Chem. Phys. Lett.* **289**, 193 (1998).
- ⁶F. Rachdi, L. Hajji, M. Galtier, T. Yildirim, J. E. Fischer, C. Goze, and M. Mehring, *Phys. Rev. B* **56**, 7831 (1997).
- ⁷G. Oszlanyi, G. Baumgartner, G. Faigel, L. Granasy, and L. Forro, *Phys. Rev. B* **58**, 5 (1998).
- ⁸O. Zhou and D. E. Cox, *J. Phys. Chem. Solids* **53**, 1373 (1992).
- ⁹P. Dahlke, P. F. Henry, and M. J. Rosseinsky, *J. Mater. Chem.* **8**, 1571 (1998).
- ¹⁰C. Gu, F. Stepniak, D. M. Poirier, M. B. Jost, P. J. Benning, Y. Chen, T. R. Ohno, J. L. Martins, J. H. Weaver, J. Fure, and R. E. Smalley, *Phys. Rev. B* **45**, 6348 (1992).
- ¹¹F. Stepniak, P. J. Benning, D. M. Poirier, and J. H. Weaver, *Phys. Rev. B* **48**, 1899 (1993).
- ¹²G. K. Wertheim, D. N. E. Buchanan, and J. E. Rowe, *Chem. Phys. Lett.* **202**, 320 (1993).
- ¹³M. Knupfer and J. Fink, *Phys. Rev. Lett.* **79**, 2714 (1997).
- ¹⁴L. Barbedette, S. Lefrant, T. Yildirim, and J. E. Fischer, in *Physics and Chemistry of Fullerenes and Derivatives*, edited by H. Kuzmany, J. Fink, M. Mehring, and S. Roth (World Scientific, London, 1995), p. 460.
- ¹⁵P. A. Heiney, J. E. Fischer, A. R. McGhie, W. J. Romanow, A. M. Denenstien, J. P. McCauley, Jr., and A. B. Smith III, *Phys. Rev. Lett.* **66**, 2911 (1991).
- ¹⁶W. I. F. David, R. M. Ibberson, J. C. Matthewman, K. Prassides, T. J. S. Dennis, J. P. Hare, H. W. Kroto, R. Taylor, and D. R. M. Walton, *Nature (London)* **353**, 147 (1991).
- ¹⁷K. Prassides, C. Christides, I. M. Thomas, J. Mizuki, K. Tanigaki, I. Hirose, and T. W. Ebbesen, *Science* **263**, 950 (1994).
- ¹⁸I. I. Khairullin, W.-T. Chang, and L.-P. Hwang, *Solid State Commun.* **97**, 821 (1996).
- ¹⁹A. R. Ramirez, *Supercond. Rev.* **1**, 1 (1994).
- ²⁰Y. Yoshida, Y. Kubozono, S. Kashino, and Y. Murakami, *Chem. Phys. Lett.* **291**, 31 (1998).
- ²¹Y. Kubozono, S. Fujiki, K. Hiraoka, T. Urakawa, Y. Takabayashi, S. Kashino, Y. Iwasa, T. Kitagawa, and Y. Mitani, *Chem. Phys. Lett.* **298**, 335 (1998).
- ²²Y. Iwasa, *Trans. Mater. Res. Soc. Jpn.* **14B**, 1085 (1994).
- ²³P. Petit, J. Robert, J.-J. Andre, T. Yildirim, and J. E. Fischer, in *Progress in Fullerene Research*, edited by H. Kuzmany, J. Fink, M. Mehring, and S. Roth (World Scientific, London, 1994), p. 478.
- ²⁴A. Janossy, O. Chauvet, S. Pekker, J. R. Cooper, and L. Forro, *Phys. Rev. Lett.* **71**, 1091 (1993).
- ²⁵T. T. M. Palstra, A. F. Hebard, R. C. Haddon, and P. B. Littlewood, *Phys. Rev. B* **50**, 3462 (1994).
- ²⁶W. A. Vareka and A. Zettl, *Phys. Rev. Lett.* **72**, 4121 (1994).
- ²⁷K. Tanigaki, M. Kosaka, T. Manako, Y. Kubo, I. Hirose, K. Uchida, and K. Prassides, *Chem. Phys. Lett.* **240**, 627 (1995).
- ²⁸P. Petit, J. Robert, T. Yildirim, and J. E. Fischer, *Phys. Rev. B* **54**, 3764 (1996).
- ²⁹R. J. Elliott, *Phys. Rev.* **96**, 266 (1954).
- ³⁰Y. Yafet, *Solid State Phys.* **14**, 1 (1963).
- ³¹J. Winter and H. Kuzmany, *Phys. Rev. B* **53**, 655 (1996).
- ³²P. Zhou, K.-A. Wang, P. C. Eklund, G. Dresselhaus, and M. S. Dresselhaus, *Phys. Rev. B* **48**, 8412 (1993).
- ³³C. M. Varma, J. Zaanen, and K. Raghavachari, *Science* **254**, 989 (1991).
- ³⁴M. Schluter, M. Lannoo, M. Needels, G. A. Baraff, and D. Tomanek, *Phys. Rev. Lett.* **68**, 526 (1992).
- ³⁵C. Taliani, V. N. Denisov, A. A. Zakhidov, G. Stanghellini, G.

- Ruani, and R. Zamboni, in *Electronic Properties of Fullerenes*, edited by H. Kuzmany, J. Fink, M. Mehring, and S. Roth (Springer-Verlag, Berlin, 1993), p. 259.
- ³⁶Y.-N. Xu, M.-Z. Huang, and W. Y. Ching, *Phys. Rev. B* **44**, 13 171 (1991).
- ³⁷M. G. Mitch, S. J. Chase, and J. S. Lannin, *Phys. Rev. Lett.* **68**, 883 (1992).
- ³⁸H. Kuzmany, T. Pichler, R. Winkler, and M. Haluska, in *Physics and Chemistry of Fullerenes and Derivatives* (Ref. 14), p. 340.
- ³⁹M. C. Martin, D. Koller, A. Rosenberg, C. Kendziora, and L. Mihaly, in *Physics and Chemistry of Fullerenes and Derivatives* (Ref. 14), p. 346.
- ⁴⁰Y. Kubozono (unpublished).
- ⁴¹J. P. Liu, *Phys. Rev. B* **49**, 5687 (1994).
- ⁴²R. Kerkoud, P. Auban-Senzier, D. Jerome, S. Brazovskii, I. Luk'yanchuk, N. Kirova, F. Rachdi, and C. Goze, *J. Phys. Chem. Solids* **57**, 143 (1996).